ELSEVIER

International Journal of Heat and Fluid Flow 22 (2001) 358–364

International Journal of HEAT AND FLUID FLOW

www.elsevier.com/locate/ijhff

MHD turbulence measurements in a sodium channel flow exposed to a transverse magnetic field

S. Eckert *, G. Gerbeth, W. Witke, H. Langenbrunner

Forschungszentrum Rossendorf (FZR), Institute of Safety Research, P.O. Box 510119, 01314 Dresden, Germany

Abstract

The influence of a static transverse magnetic field on a turbulent sodium flow in a channel with a rectangular cross-section is investigated. The turbulence has been forced by mechanical means employing a grid of cylindrical bars. Electric potential probes have been used to determine the longitudinal component of the liquid velocity. The experiments cover a wide range of the non-dimensional parameters Hartmann number ($Ha \leqslant 3000$) and the magnetic interaction parameter ($N \leqslant 800$). Measurements of the turbulence intensity as a function of the magnetic interaction number N will be presented and discussed. The measured spectra are essentially different from those predicted according to the theory of two-dimensional turbulence.

Keywords: MHD turbulence; Liquid metal channel flow; Transverse magnetic field; Local velocity measurements; Potential probes; Velocity profiles; Turbulence intensity; Power spectra

1. Introduction

The turbulence characteristics in liquid metal flows are considerably changed if the flow is exposed to an external magnetic field. It is well known that the application of a static magnetic field tends to damp the turbulent motion in an electrically conducting fluid. However, several experimental studies (Branover et al., 1965; Hua and Lykoudis, 1974; Votsish and Kolesnikov, 1976) revealed that the effect of a transverse magnetic field on a turbulent liquid metal flow does not lead exclusively to a suppression of the turbulent perturbations. As shown by Sommeria and Moreau (1982) vortices are weakly damped if their axes are aligned with the magnetic field lines resulting from the anisotropic character of the electromagnetic dissipation term. Consequently, the character of the flow shows a distinct anisotropy with the tendency to become two-dimensional. The properties of the local mass transfer investigated by Kolesnikov and Tsinober (1974) and Eckert et al. (2000) are strongly governed by the anisotropic character of the flow.

It was also demonstrated by Sommeria and Moreau (1982) that the existence of rigid, electrically insulating boundaries perpendicular to the magnetic field lines is responsible for the so-called Hartmann effect resulting in a change of the velocity profile and formation of thin Hartmann layers at the wall. Obviously, the flow cannot become purely two-dimensional in such a configuration.

In our experiments the decaying turbulent motion of liquid sodium behind a grid of cylindrical rods in a transverse magnetic field was investigated. Velocity measurements behind a grid of cylindrical rods parallel to an external transverse magnetic field were performed by Kolesnikov and Tsinober (1972). It was found that the spectra contained intervals, being described by a k^{-3} law in the high-frequency part of the spectrum and by a $k^{-5/3}$ law at lower frequencies. The results were interpreted as an indicator for the existence of an inverse energy cascade known from the theory of two-dimensional turbulence. The influence of an external magnetic field on homogeneous turbulence was shown experimentally by Alemany et al. (1979). An almost isotropic turbulence was generated in stagnant mercury by a grid moving along the channel. Here, the magnetic field was directed parallel to the channel walls. The results show a $t^{-1.7}$ law for decay of the turbulent energy and a k^{-3} slope in the kinetic energy spectrum. The authors explain the observations with the balance between the Joule dissipation and the non-linear angular energy transfer. Branover et al. (1994) carried out an experimental study related closely to the present paper. Velocity fluctuation spectra have been measured in a turbulent mercury flow behind a honeycomb under the influence of an imposed transverse magnetic field. The authors found a dependence of spectral exponents on the value of the magnetic interaction parameter. Therefore, they suggest the existence of four different turbulent modes in their experiments with well-distinguished characteristic exponents $k^{-\alpha}$, where $\alpha = 5/3$, 7/3, 3 and 11/3.

* Corresponding author. Tel.: +49-351-260-2132; fax: +49-351-260-2007.

E-mail address: s.eckert@fz-rossendorf.de (S. Eckert).

0142-727X/01/$ - see front matter
PII: S0142-727X(01)00099-6

Crucial parameters to describe MHD flows are the Hartmann number Ha as a ratio between electromagnetic and viscous forces and the magnetic interaction parameter N as a ratio between electromagnetic and inertial forces:

$$Ha = BL\sqrt{\frac{\sigma_l}{\rho\nu}}, \tag{1}$$

$$N = \frac{\sigma_l LB^2}{\rho V} = \frac{Ha^2}{Re}, \tag{2}$$

where $B, L, V, \rho, \sigma_l, \nu$ stand for the magnetic field induction, typical length scale, typical velocity scale, density, electrical conductivity, and kinematic viscosity of the fluid, respectively. The present measurements were performed in a parameter range ($Ha \gg 1$, $N > 1$), where the local structure of the turbulent sodium flow is strongly influenced by the applied magnetic field.

2. Experimental set-up, measuring technique and data processing

The following section provides a brief view of the experimental equipment. A more detailed description of the experiment as well as a discussion about the reliability of the used measuring technique is given by Eckert (1998).

The experiments have been carried out in the FZR sodium facility with two different test sections in the following denoted as versions A and B. Both experimental situations are compared in Table 1. The mean flow is generated by an electromagnetic pump and passes a transverse magnetic field (length: 320 mm, $B_{\max} = 0.45$ T).

With the test section A the most simple channel configuration is realized. The channel walls made of stainless steel (electrical conductivity σ_w) have a thickness of $\delta_w = 5$ mm resulting in a wall conductance ratio $c_w = \sigma_w \cdot \delta_w/\sigma_l \cdot a$ of 0.026. Table 1 also shows the ratio of the electrical resistance of the Hartmann layer characterized by a typical thickness $\delta_{Ha} = a/Ha$ and the channel wall $R_{Ha}/R_w = \sigma_l \cdot \delta_{Ha}/\sigma_w \cdot \delta_w = Ha \cdot c_w$. This quantity becomes larger than one for a Hartmann number of 150 resulting from the minimum magnetic field strength of 0.05 T adjusted in the present experiment. Here, the channel walls have to be considered as electrically conducting. A grid of cylindrical bars was positioned at the beginning of the homogeneous magnetic field region to generate the turbulence. The cylinders are rotatably mounted, so that the angle between the direction of the cylinder axes and the magnetic field lines can be modified.

A special ensemble of channel inserts was employed in the experiments with test section B. The objectives were to

- Suppress the development of the characteristic M-shaped velocity profile of MHD channel flows (Moreau, 1990),
- Damp the turbulent perturbations arising from the flow entry effects into the magnetic field region.

To decrease the wall conductance ratio the inner wall of the rectangular channel cross-section was covered by a U-shaped insert (see Fig. 1) consisting of two thin stainless steel sheets (thickness 0.2 mm). An electrically insulating layer is enclosed by these metal sheets welded along the edges. The c_w-value of the insert is about 0.0012 and consequently more than 10 times lower compared with the ordinary channel wall. The reason to use a U-shaped insert is caused by the requirement to have a free side to be able to install local probes.

The ensemble of channel inserts is completed by the following components (see also Fig. 2):

- Two honeycombs (1) installed at the fringe field regions in order to avoid the generation of the typical M-shaped velocity profile,

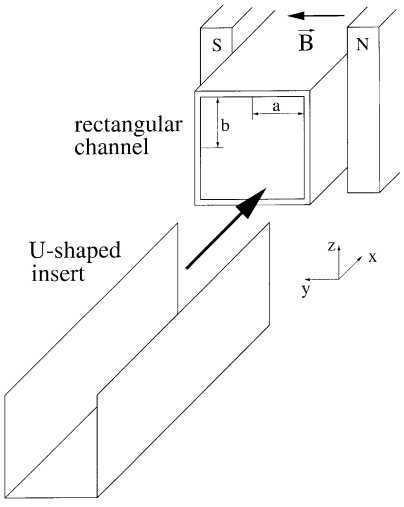

Fig. 1. Scheme of the U-shaped insert positioned at the inner channel wall of test section B.

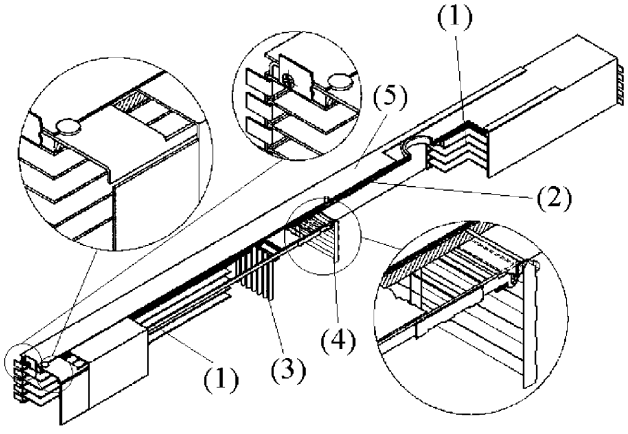

Fig. 2. Sectional view of the channel inserts installed in test section B.

Table 1
Details of both test sections A and B

	Test section A	Test section B
Cross-sectional area	45×50 mm^2	45×45 mm^2
Wall material	Stainless steel	Stainless steel
Wall thickness	5 mm	0.2 mm (special wall covering)
c_w	0.026	0.0012
R_{Ha}/R_w ($Ha = 150$)	3.9	0.18
Channel inserts	Turbulence promoter	Ensemble of inserts (see Fig. 2)

- A 3 mm copper plate (2) located at the wall in front of the free side of the U-shaped (5) insert to reach a better homogenization of the flow,
- A grid of copper (3) bars aligned perpendicular to the direction of the magnetic field to suppress the remaining turbulence arising at the outlet of the first honeycomb and
- A grid of steel sheets parallel to the field lines acting as turbulence promoter (4).

The longitudinal component of the velocity and its fluctuations have been measured by means of two-electrode potential probes as shown in Fig. 3. The local probes are connected with a traversing system allowing to move the sensor in the cross-sectional area. The function of the potential-difference probe is governed by Ohm's law in moving fluids.

$$\frac{\vec{j}}{\sigma_l} = -\nabla\phi + \vec{u} \times \vec{B}. \tag{3}$$

For MHD channel flows characterized by high Hartmann numbers and a small wall conductance ratio $((1/Ha) \ll c_w \ll 1)$ the total current density $\vec{j}$ in the bulk flow can be neglected compared to the induced one

$$|\vec{j}| \ll \sigma_l |\vec{u} \times \vec{B}|. \tag{4}$$

As a consequence, the measured electric potential drop $\Delta\phi$ between the electrodes, spatially separated by the distance l, has the following simple dependence on the fluid velocity u

$$\Delta\phi = B \cdot l \cdot u. \tag{5}$$

The choice of the distance l at the sensor tip is a compromise between the magnitude of the signals and the ability to resolve the small scales of the spectrum. The limited spatial resolution of the probe acts in fact as an additional low-pass filter. Thus, the measured spectra have to be corrected to exclude the distortions caused by the spatial averaging process. To correct the measured turbulence spectra Bolonov et al. (1976) suggested to apply a special function extracted from turbulence measurements by means of potential probes with different electrode distances varying between 1.5 and 20 mm. This correction function has also been used in the present paper. A detailed discussion about this problem and a description of the applied method have been given by Eckert (1998). The distance between the electrodes of the potential probes in the present experiment was chosen as 1 mm.

To aquire the probe signal a DAS1600 data aquisition board (Keithley) connected with a home-made low-noise preamplifier has been used. The electronic equipment has a maximum accuracy of 0.488 μV which gives us for a magnetic field of 0.2 T and $l = 1$ mm a velocity resolution of about 2.4 mm/s. A sample rate of 700 Hz or 2 kHz was chosen. The presented power spectral densities were calculated from the ratio of the fluctuation and the mean signal by direct FFT. For this reason the data records were subdivided into time windows of 8192 points corresponding to measuring times of about 11 and 4 s, respectively, and resolutions with respect to the frequency of 0.085 and 0.25 Hz, respectively. The power spectral densities were finally obtained by an ensemble averaging based on 87 data records with an overlapping of 75%. Using the well-known Taylor hypothesis, the corresponding wave numbers have been received. The presented values of the turbulence intensity tu are obtained from measurements of the mean streamwise velocity component U and the local velocity fluctuation u' according to the following relation:

$$tu = \frac{u'}{U}, \quad u' = \left[\frac{1}{M-1}\sum_{m=1}^{M}(u_m - U)^2\right]^{1/2}, \tag{6}$$

where M denotes here the total number of the sampled velocity values.

3. Experimental results

Profiles of the velocity and the turbulence intensity measured in both test sections A and B perpendicular to the magnetic field without turbulence promoter are displayed in Figs. 4 and 5, respectively. A pronounced M-shape has been observed in the test section A without channel inserts. On the other hand, utilization of the channel inserts in the test section B results in a distinct smoothing of the profile. Although a slight increase of velocity near the channel wall has also to be noted, the enhancement does not exceed 10% with respect to the mean velocity U. Without using a grid as turbulence

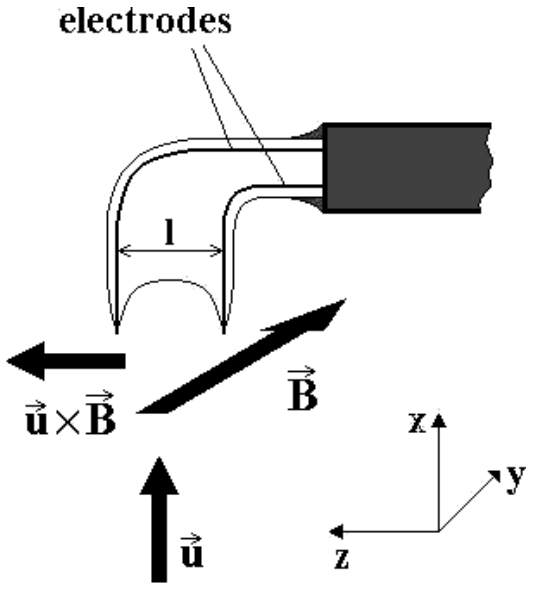

Fig. 3. Principle of the two-electrode potential-difference probe.

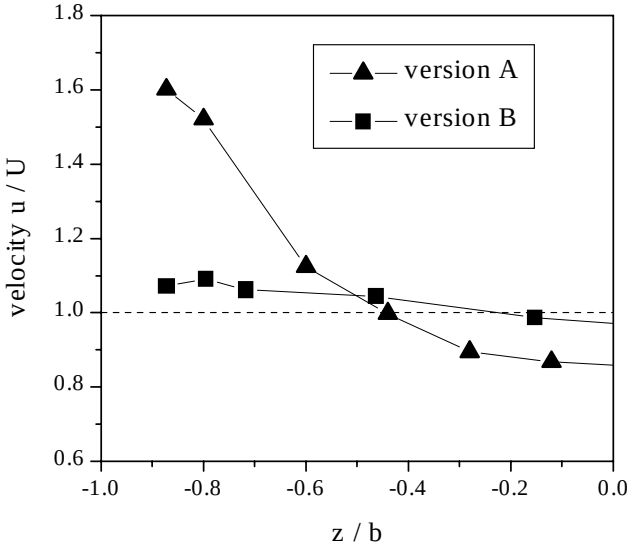

Fig. 4. Velocity profiles measured perpendicular to the magnetic field in the test section A ($Re = 46\,500$, $Ha = 1500$, $N = 48$) and B ($Re = 16\,300$, $Ha = 1000$, $N = 61$), respectively.

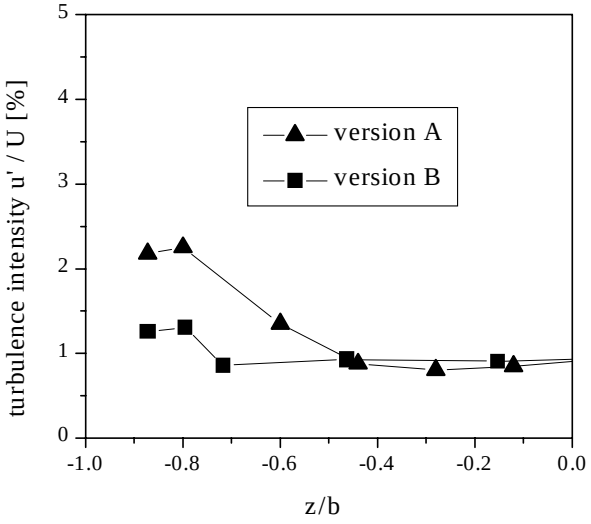

Fig. 5. Profiles of the turbulence intensity measured perpendicular to the magnetic field in the test section A ($Re = 46\,500$, $Ha = 1500$, $N = 48$) and B ($Re = 16\,300$, $Ha = 1000$, $N = 61$), respectively.

promoter the turbulence intensities were not larger than 3% for any measurement in the test sections A or B. The increase of the turbulence level near the channel wall in test section A is caused by the presence of velocity jets of the M-shaped profile. For a more detailed presentation of these results we refer the reader to Eckert (1998).

The turbulence intensity will be discussed as a function of the magnetic interaction parameter N. The potential-difference probe was positioned in the centre of the cross-sectional area 290 mm behind the entrance of the flow into the region of the uniform magnetic field. The results obtained for both versions without turbulence promoter are shown in Fig. 6. For $N < 10$ turbulence intensities of about 3% were found. A further increase of the magnetic interaction parameter results in a monotonous decrease of the turbulence intensity to values less than 1%.

The case with the turbulence generating grid is depicted in Fig. 7. The cylinders of the grid were aligned with the magnetic field lines. Here, the turbulence intensity increases with growing magnetic interaction parameter up to a maximum located at about $N = 70$ (version A) and $N = 120$ (version B). The

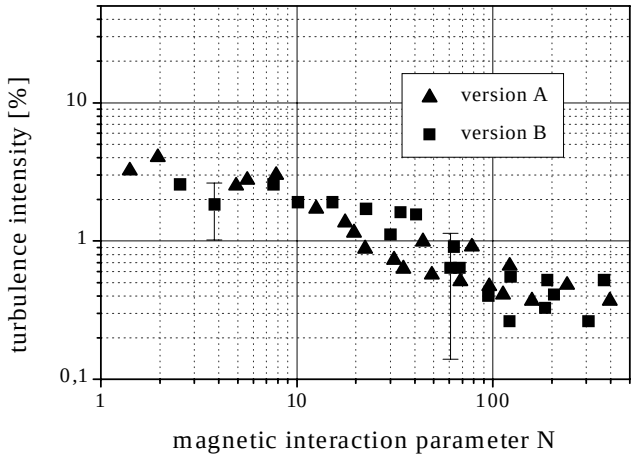

Fig. 6. Turbulence intensity as a function of the magnetic interaction parameter N obtained without turbulence promoter.

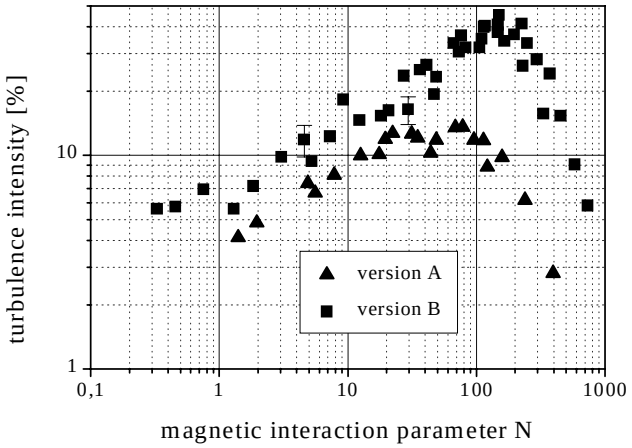

Fig. 7. Turbulence intensity as a function of the magnetic interaction parameter N obtained with installed turbulence promoter.

reduction of the wall conductance ratio by a factor of about 25 results in a significant enhancement of the turbulence level by a factor of 2–5 as well as in a shift of the observed maximum of the turbulence intensity towards larger values of N.

These observed tendencies also become obvious in the obtained power spectra. A selection of the power spectra obtained in the test section B without and with installed turbulence promoter is shown in Figs. 8 and 9, respectively. A drastic damping of the turbulent kinetic energy with increasing N has to be registered in the case without turbulence promoter, while an enhancement of the spectral energy can be observed if the turbulizing grid has been installed. Moreover, as revealed by Fig. 9 the spectral slope of the inertial region becomes steeper with growing N. The exponents of the slope extracted from the power spectra which have been obtained in test section B are drawn in Fig. 10 versus the magnetic interaction parameter N. For small values $N \leqslant 1$ we found a $k^{-5/3}$ law according to the Kolmogorov theory for isotropic turbulence. A further increase of N results in a monotonous decrease of the spectral exponents up to a minimum located at $N \approx 120$, obviously an inverse behaviour as already found for the turbulence intensity in Fig. 7.

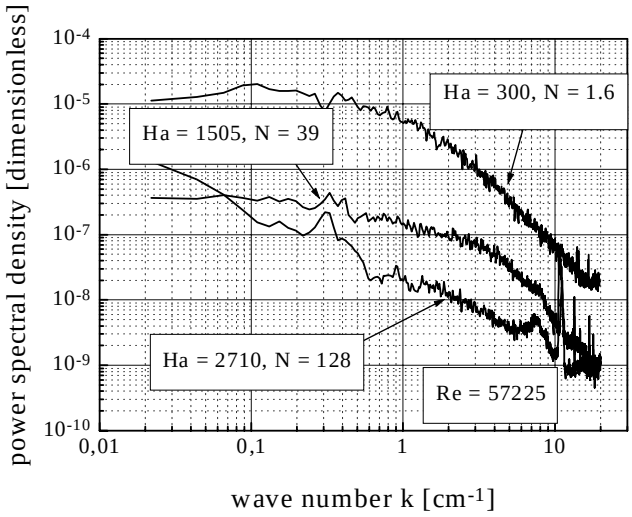

Fig. 8. Power spectra obtained in test section B without turbulence promoter at $Re = 57\,225$.

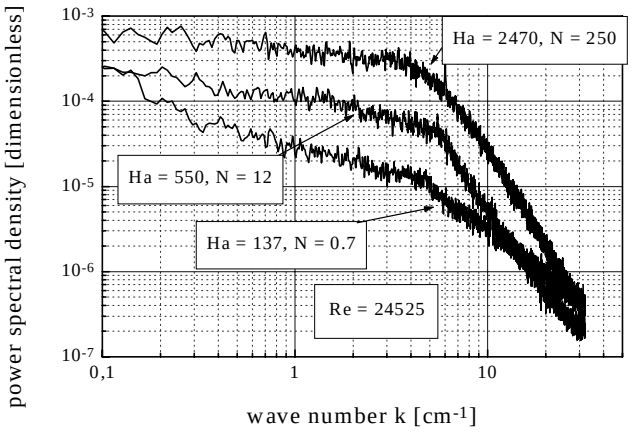

Fig. 9. Power spectra obtained in test section B with installed turbulence promoter at $Re = 24\,525$.

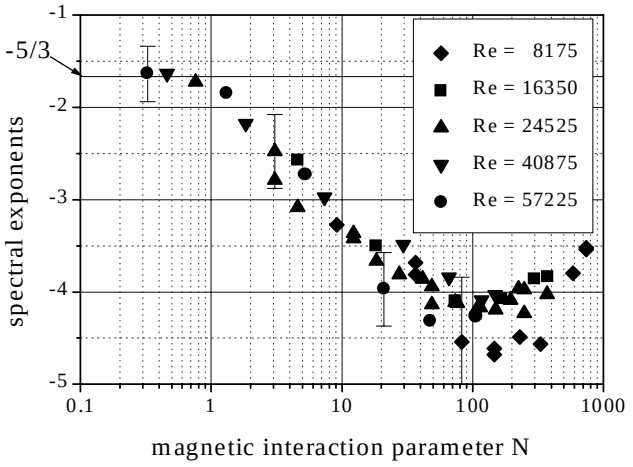

Fig. 10. Spectral exponents as a function of the magnetic interaction parameter N obtained in the test section B.

4. Discussion and conclusions

The generation of vortices at different kinds of grids in a flow imposed to a transverse magnetic field was investigated by Kljukin and Kolesnikov (1989). If the magnetic field is sufficiently strong a high correlation of velocity signals was measured close to a grid of cylinders aligned with the direction of the external magnetic field. The authors suggest a synchronization of the vortex shedding by the magnetic field effect resulting in the generation of quasi-two-dimensional wakes and finally of quasi-two-dimensional vortices due to the mechanism of the electromagnetic diffusion of the vorticity as found by Sommeria and Moreau (1982). The quasi-two-dimensional vortices may become unstable and decay in three-dimensional structures which will be damped quickly due to the Joule dissipation with the typical time scale

$$\tau_j = \frac{\rho}{\sigma B_0^2}. \tag{7}$$

The application of a strong magnetic field prevents the onset of the three-dimensional instabilities and conserves therefore the kinetic turbulent energy. The increase of the turbulence intensity with increasing magnetic interaction parameter N as shown in Fig. 7 can be explained by the existence of such a mechanism.

The decrease of the turbulence intensity at large values of $N > 120$ as shown in Fig. 7 is caused by the fact that the channel walls do not consist of electrically insulating material. The vortices extended over the full channel size along the magnetic field will not be directly affected by the Joule dissipation. If the channel walls are perfectly insulating, the induced electrical current can only circulate in the Hartmann layer. Consequently, the dissipation process is governed by the Hartmann effect characterized by the time scale

$$\tau_{Ha} = \left(\frac{\rho}{\sigma\nu}\right)^{1/2} \frac{a}{B_0}. \tag{8}$$

A comparison between both time scales shows: $\tau_{Ha} \ll \tau_j$. However, the dissipation also becomes significant for the quasi-two-dimensional structures if the channel walls are electrically conducting. At sufficiently high Hartmann numbers the electrical resistance of the Hartmann layers may become much larger as compared with the conducting channel wall. The resulting reduction of the electrical resistance leads to the closure of strong electrical currents. Consequently, the kinetic energy of the vortices is transferred to electrical energy and finally dissipated by the Joule effect. This explanation is confirmed by the graphs in Fig. 7 showing for the reduced wall conductance ratio in test section B significant higher turbulence intensities as well as a shift in the maximum of the curve $tu(N)$ to higher values of the magnetic interaction parameter.

The previous argumentation is based on the assumption that the kinetic energy is concentrated in quasi-two-dimensional eddies which span the whole channel width $2 \cdot a$. Indeed, this assumption is confirmed by several experimental results performed by Eckert (1998). Here, we cannot discuss all the details, but, deliver some plausible arguments. Sommeria and Moreau (1982) argued that a turbulent eddy of the scale $l_\perp$ perpendicular to the magnetic field has a length

$$l_\parallel = \sqrt{N_l} l_\perp \tag{9}$$

in the direction of the magnetic field. Here, N_l denotes the magnetic interaction parameter based on the scale $l_\perp$

$$N_l = \frac{\tau_{\mathrm{tu}}}{\tau_j} = \frac{\sigma B^2 l_\perp}{\rho u}. \tag{10}$$

Assuming a locally isotropic turbulence in the plane perpendicular to the magnetic field lines we can write the eddy-turnover time as follows (Landau and Lifschitz (1991))

$$\tau_{\mathrm{tu}} = \frac{l}{u} = \left(\frac{2\pi}{k}\right)^{2/3} \frac{(2 \cdot a)^{1/3}}{u}. \tag{11}$$

This gives us the possibility to express N_l as a function of the wave number k. With $l_\perp = 2\pi/k_\perp$ Eq. (9) can be transformed into

$$l_\parallel = \left(\frac{2\pi}{k}\right)^{4/3} B \sqrt{\frac{\sigma(2 \cdot a)^{1/3}}{\rho u^{4/3}}} \tag{12}$$

Calculated results for $l_\parallel(k)$ obtained at a Reynolds number of 65,100 for different values of the Hartmann number are displayed in Fig. 11. Fig. 12 shows the power spectral densities measured at the same Reynolds and Hartmann numbers in the test section A. We want to focus our interest on the transition point between the energy and the inertial range which is obviously shifted towards higher wave numbers with growing Hartmann number. This transition region can be approximately localized at the same wave numbers as found in Fig. 11 for the condition $l_\parallel = 2 \cdot a$ allowing the interpretation that the kinetic energy is concentrated in quasi-two-dimensional eddies

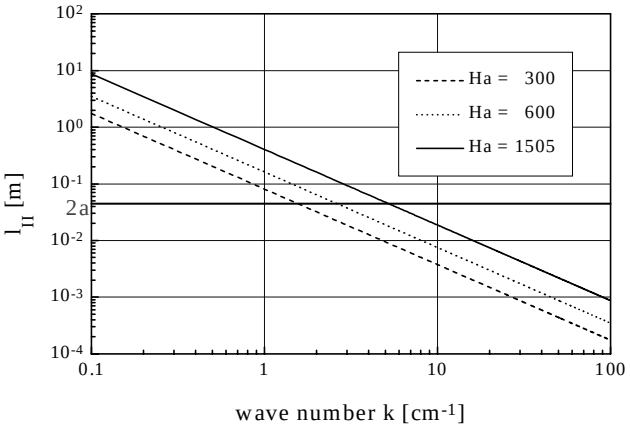

Fig. 11. Calculated scale of the turbulent eddies along the magnetic field as a function of the wave number k.

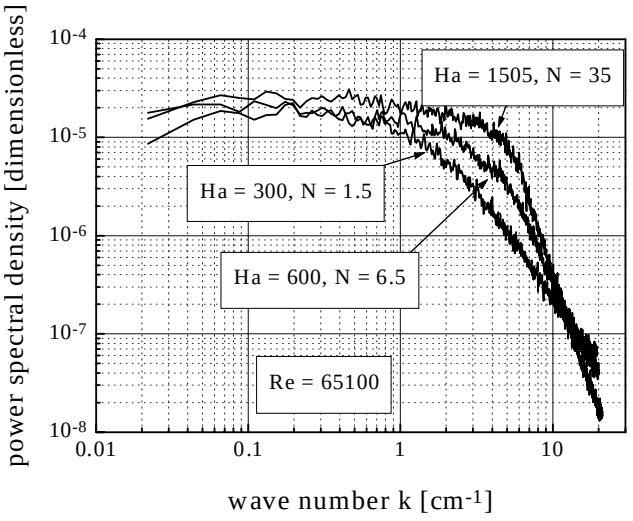

Fig. 12. Power spectra obtained in test section A with installed turbulence promoter at $Re = 65100$.

governed by the Hartmann effect whereas smaller three-dimensional eddies at higher wave number will be dissipated by the Joule effect.

Moreover, according to Eq. (9) we would expect a decreasing behaviour of the scale $l_\perp$ with growing magnetic interaction parameter if $l_\parallel$ is considered to be identical with the channel width $2 \cdot a$ (quasi-two-dimensional case). Fig. 13 depicts the measured integral scale versus N. The monotonous decrease of the integral scale with increasing magnetic interaction indicates the expected reduction in the mean size of the energy containing eddies.

As shown in Fig. 10 we have observed a decreasing spectral exponent with increasing interaction parameter N starting from the well-known value of $-5/3$ up to a minimum of -4. It is difficult to explain this fact within the frame of the 2D turbulence model by Kraichnan (1967) predicting a k^{-3}-law. Spectral exponents which differ from the values of $-5/3$ and -3 were also found in the experiments by Branover et al. (1994). A 3D helical model for the analysis of turbulent MHD flows is suggested by Branover et al. (1999). The existence of decay laws $k^{-\alpha}$ with $-7/3$, $-11/3$ and -4 is explained by the generation of helicity in MHD flows. The $-7/3$ slope is connected with a transfer of helicity whereas the values of $-11/3$ and -4 will be observed if the helical turbulence becomes intermittent.

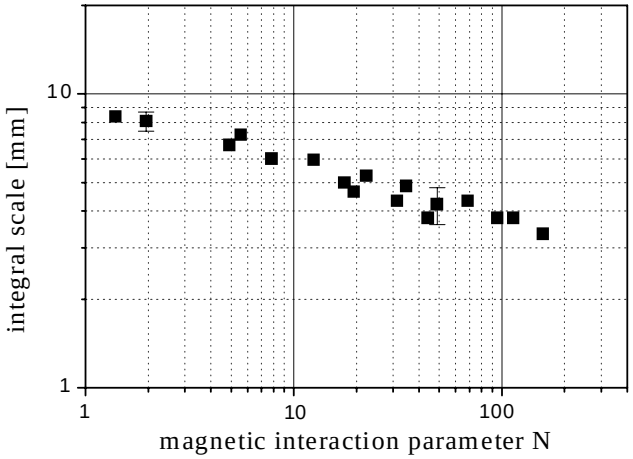

Fig. 13. Integral scale as a function of the magnetic interaction parameter N obtained in test section A at $Re = 65100$.

The spectral exponents derived from our experiments show a monotonous decrease with growing N. The uncertainties of the measurement may have to be considered as the reason why our results did not exactly coincide with the discrete values predicted by Branover et al. (1999).

The evaluation of the experimental results allows the following conclusions:

- The flow structure is dominated by the existence of quasi-two-dimensional vortices extended along the magnetic field lines and limited in size by the Hartmann walls. These vortices contain the turbulent kinetic energy of the flow.
- The dissipation of the turbulent energy is strongly influenced by the electrical conductivity of the channel wall.
- The quasi-two-dimensional turbulent structures arising from the wake of a grid consisting of cylinders are stabilized by the influence of an external transverse magnetic field if the cylinders are aligned parallel to the magnetic field lines.
- The exponents characterizing the slope of the inertial range in the power spectra are changed by a variation of the magnetic interaction parameter N. In contradiction to the results of Branover et al. (1994) we did not find several discrete values of the spectral exponents identifying different modes of the quasi-two-dimensional turbulence. The spectral slope becomes steeper rather monotonously with growing N starting with a $k^{-5/3}$ law for $N \leqslant 1$ and reaching a minimum of the spectral exponents of about -4 for $N \approx 120$.

Acknowledgements

This work was supported by the Deutsche Forschungsgemeinschaft under contract Ge 682/4-3. Furthermore, the authors would like to express their thanks to I. Platnieks and O. Lielausis for the fruitful discussions as well as for their valuable support in preparing the ensemble of channel inserts.

References

Alemany, A., Moreau, R., Sulem, P.L., Frisch, U., 1979. Influence of an external magnetic field on homogeneous MHD turbulence. J. de Mechanique 18, 277–313.

Bolonov, N., Charenko, A., Eidelmann, A., 1976. About the correction of turbulence spectra measured by conduction anemometer. Ing. Phys. J. 2, 243–247 (in Russian).

Branover, H.H., Slyusarev, N.M., Sherbinin, E.V., 1965. Some results of measuring turbulent pulsation of velocity in a mercury flow in the presence of a transverse magnetic field. Magn. Gidrodin. 1, 33–41 (in Russian).

Branover, H., Eidelmann, A., Golbraikh, E., Moiseev, S.S., 1999. Turbulence and Structures. Academic Press, New York.

Branover, H., Eidelmann, A., Nagorny, M., 1994. Quasi-two-dimensional helical turbulence in MHD and geophysical flow. Proceedings of the Second International Conference on Energy Transfer in Magnetohydrodynamic Flows 2, 777–785.

Eckert, S., 1998. Experimentelle Untersuchung turbulenter Flüssigmetall- und Flüssigmetall-Gas Strömungen in einem äußeren Magnetfeld. Report FZR-219.

Eckert, S., Gerbeth, G., Lielausis, O., 2000. The behaviour of gas bubbles in a turbulent liquid metal MHD flow – Part I: Dispersion in quasi-two-dimensional turbulence. J. Multiphase Flow 26, 45–66.

Hua, H.M., Lykoudis, P.S., 1974. Turbulence measurements in a magneto-fluid-mechanic channel. Nucl. Sci. Eng. 3, 445–449.

Kljukin, A., Kolesnikov, Y.B., 1989. MHD turbulence decay behind spatial grids. In: Lielpeteris and Moreau (Eds.), Liquid Metal Magnetohydrodynamics. Kluwer Academic Publisher, Dordrecht, Boston, London, pp. 153–159.

Kolesnikov, Y.B., Tsinober, A.B., 1972. An experimental study of two-dimensional turbulence behind a grid. Fluid Dynamics 9, 621–624.

Kolesnikov, Y.B., Tsinober, A.B., 1974. An experimental study of two-dimensional turbulence behind an array. Mekhanika Zhidkosti i Gasa 4, 146–151 (in Russian).

Kraichnan, R.H., 1967. Inertial ranges in two-dimensional turbulence. Phys. Fluids 10, 1417–1423.

Landau, L.D., Lifschitz, E.M., 1991. Lehrbuch der Theoretischen Physik: Bd. VI Hydrodynamik. Akademie Verlag, Berlin.

Moreau, R., 1990. Magnetohydrodynamics. Kluwer Academic Publishers, Dordrecht, Boston, London.

Sommeria, J., Moreau, R., 1982. Why, how and when MHD turbulence becomes two-dimensional. J. Fluid Mech. 118, 507–518.

Votsish, A.D., Kolesnikov, Y.B., 1976. Spatial correlation and vorticity in two-dimensional turbulence. Magn. Gidrodin. 3, 25–28 (in Russian).